Aerodynamic Characteristics and Flow Round Cross Parachutes in Steady Motion

C. Q. Shen* and D. J. Cockrell†
The University of Leicester, Leicester, England, United Kingdom

Because of their simplicity of manufacture as well as the excellence of their drag and stability characteristics, cross-parachute canopies are widely applied, particularly where their propensity to rotate is not an important design feature. Making extensive force measurement and flow visualization tests in a wind tunnel and also conducting blockage effect experiments under water in a large cross-sectional area ship tank using the same cross-shaped canopy models, the authors considered the physical reasons for these aerodynamic characteristics. It was already known that the arm ratio of the canopy is a significant aerodynamic parameter in the determination of its drag and stability characteristics, and their tests showed that the porosity of the canopy fabric is equally important. Physical reasons are advanced for the importance of these two parameters and recommendations are made as to their best choice in a given application.

Nomenclature

A = canopy arm ratio $A = L/W$
C_M = aerodynamic pitching moment coefficient
C_N = normal or side force aerodynamic coefficient
C_T = tangential or axial aerodynamic force coefficient
D_o = nominal diameter of the parachute canopy $D_o = (4S_o/\pi)^{1/2}$
L = arm length of a cross-shaped canopy
ℓ = distance of the tuft grid downstream of the canopy apex
ℓ_s = length of the canopy suspension line
R = total aerodynamic reaction on canopy
R_s = suspension line ratio $R_s = \ell_s/L$
S_o = nominal total surface area of the canopy for cross parachutes $S_o = W(2L - W)$
S_p = projected frontal area of the inflated canopy
V = resultant relative velocity of air or water
W = arm width of a cross-shaped canopy
α = angle of attack
λ = nominal canopy porosity
ρ = density of the air or water in which the canopy is immersed

Subscripts

o = at zero angle of attack
c = at the suspension line confluence point
col = at canopy collapse angle of attack
eq = condition for equilibrium and static stability
p = at the center of pressure

Introduction

BECAUSE of their relatively high drag coefficients and low manufacturing costs, cross (or cruciform) parachutes are widely used aerodynamic decelerators. Cross parachutes with arm ratios that are greater than 3 : 1 display excellent stability characteristics in pitch.

Structural nonuniformities that occur can cause any parachute canopy with a symmetrical configuration to rotate about its axis of symmetry. Cross parachute canopies, having four large air gaps formed between their arms, will very readily rotate. Because of these air gaps, Jorgensen[1] proposed that the aerodynamic behavior of cross parachutes depends solely on their arm ratios, and any effects caused by their fabric porosity are not important. For cross parachute canopies having an arm ratio of 3.79 : 1, Ludtke[2] found significant effects on spinning characteristics when he varied both this fabric permeability and the lengths of the suspension lines. However, little is known about the physical reasons why fabric porosity, arm ratio, and suspension line ratio should affect the aerodynamic characteristics of cross parachutes.

Using force measurements and flow visualization in both a wind tunnel and a large ship tank to investigate these phenomena at Reynolds numbers (based on canopy nominal diameter D_o) that varied from 1.0×10^5 to 5.0×10^5, the authors recently have tested a family of cross parachute model canopies having different arm ratios L/W, suspension line length ratios ℓ_s/L, and fabric porosities λ, these terms being illustrated in Fig. 1. Measurements presented in this paper indicate that both the arm ratio and the fabric porosity have

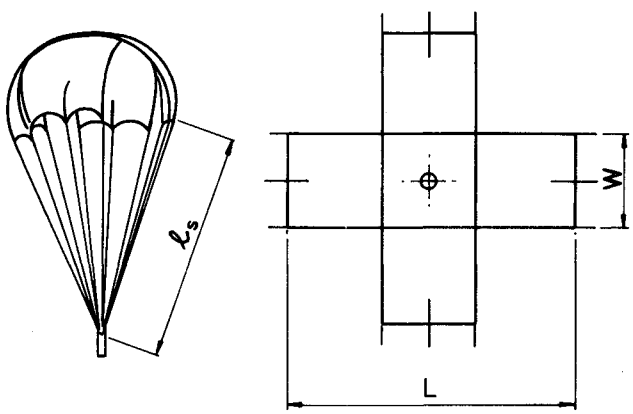

Fig. 1 Configuration of the cross parachute models.

Presented as Paper 86-2458-CP at the AIAA 9th Aerodynamic Decelerator and Balloon Technology Conference, Albuquerque, NM, Oct. 7-9, 1986; received Dec. 4, 1986; revision received Aug. 12, 1987.

*Honorary Visiting Fellow, Engineering Department; currently with the Research Institute of the Hongwei Machinery Factory, Xiangfan, Hubei Province, China. Member AIAA.
†Senior Lecturer. Member AIAA.

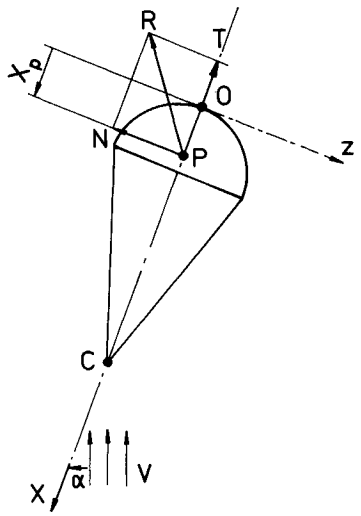

Fig. 2 Coordinate system for parachute.

Table 1 Characteristics of canopies tested

Arm Ratio $A = L/W$	Suspension Line Ratio $R_s = \ell_s/L$	Nominal Porosity λ $ft^3/ft^2/s$ at 10 in. of water pressure differential
2.4; 3.0; 4.0	0.67; 1.33; 2.00	0; 13; 23

important effects on the aerodynamic characteristics of cross parachutes.

Taneda[3] has discussed the ways in which vortices are developed in the wake formed behind a sphere immersed in a steadily flowing fluid. Bearman and Trueman,[4] as well as Nakamura and Ohya[5] have visualized the flow around rectangular blocks and square prisms. Parachute canopies at zero angle of attack are also symmetric bluff bodies which give rise to flow patterns, thus to aerodynamic forces, not unlike those developed around these other bluff bodies. Knacke[6] and others have mistakenly considered the flow around a body of revolution such as a parachute canopy to be similar to that around a long circular cylinder, which periodically sheds vortices into its wake. However, the flow around even a hemispherically shaped parachute canopy is a much more complex phenomenon than Knacke's sketches would indicate.

Experimental Program

Twenty-seven flexible cross canopy parachute models in all were investigated, possessing a nominal surface area, S_o, of 0.108 m^2(1.16 ft^2). Their canopies were made of nylon, and twelve suspension lines were attached to the skirt of each canopy. For the purposes of mounting and aerodynamic force measurement on each parachute model, a metal sting ran from the suspension line confluence point and through an eyelet in the canopy crown. So that the attitude of the canopy could be set and the aerodynamic forces developed on the canopy could be determined, this sting was rigidly fixed to the wind tunnel or the ship tank balance mechanism. This mounting method can be used to prevent any canopy spin which could result from manufacturing nonuniformities. Inevitably, the sting must cause some distortion of the canopy, particularly at high angles of attack, but by choice of an appropriate eyelet size this distortion can be minimized. The various characteristics of the canopies tested are given in Table 1.

A coordinate system fixed to the canopy is adopted, and this is shown in Fig. 2. The origin, 0, is located at the canopy crown with the axis 0-x coinciding with the axis of symmetry. The conventionally positive directions of the aerodynamic force components T and N are in the opposite sense to the positive directions of the axes 0-x and 0-z respectively. The

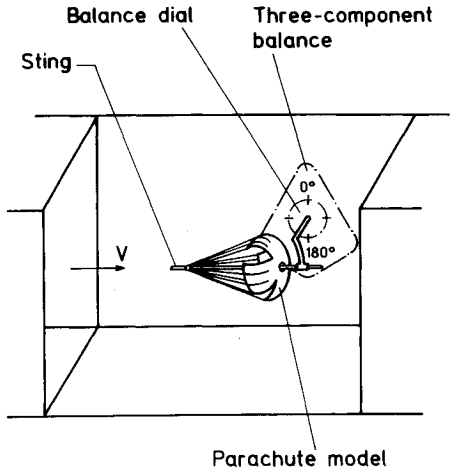

Fig. 3 Model suspension for force measurement.

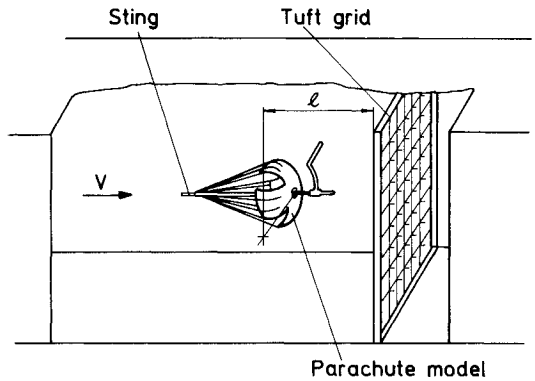

Fig. 4 Experimental arrangement for wool-tuft visualization.

center of pressure P is that point on the axis of symmetry through which the total aerodynamic reaction R acts and is at a distance x_p from the origin. The normal force component N causes an aerodynamic pitching moment $M_c = -(x_c - x_p)N$ about the suspension line confluence point C. Since the latter is located close to the centroid for the parachute and payload system, the pitching moment coefficient about this confluence point is effectively that about the system's centroid.

Measurement of the Aerodynamic Forces and Moments

Wind tunnel measurements were made in a horizontal return flow wind tunnel with a closed working section having a cross-sectional area of 1.14 m × 0.84 m (3.75 × 2.75 ft). The arrangement adopted for the canopy models, mounted via their supporting stings onto a three-component balance is shown in Fig. 3.

Amplified signals from strain gages mounted on the balance arms and from a pressure transducer detecting the working section dynamic pressure were fed to a microcomputer, the latter being used to determine and display as functions of the angle of attack the aerodynamic coefficients C_T, C_N and C_{Mc}.

Flow Visualization

Flow visualization tests were conducted in the same facility used for force measurements. At Reynolds numbers of between 1.0×10^5 and 2.0×10^5 both wool tufts and neutral buoyancy soap bubbles were used to visualize the flowfield surrounding the canopy. Wool tufts were attached to each nodal point of a wire frame having a pitch of 25 mm (1 in.), the frame being located in the wake downstream of the canopies, as shown in Fig. 4.

The arrangement adopted for the neutrally buoyant, helium-filled soap bubbles is seen in Fig. 5, in which the head

Table 2 Summary of aerodynamic behavior for cross parachutes

Arm ratio $A = L/W$	Porosity (ft³/ft²/s)	Suspension line ratio $R_s = \ell_s/L$	Canopy area $S_o(m^2)$	Canopy area $S_p(m^2)$	Tangential force coefficient (at $\alpha = 0$ deg) C_{To}: Wind tunnel test	Tangential force coefficient (at $\alpha = 0$ deg) C_{To}: Corrected by Maskell's method	Tangential force coefficient (at $\alpha = 0$ deg) C_{To}: Ship tank test	α_{eq} deg	$(\frac{dC_{Mc}}{d\alpha})_{\alpha=0\,deg}$	Collapse angle of attack α_{col}
4.0	0	2.00	0.106	—	1.01	—	—	0	< 0	—
4.0	0	1.33	0.106	0.078	0.92	0.74	0.79	0	< 0	—
4.0	0	0.67	0.106	—	0.77	—	—	0	< 0	—
4.0	13	2.00	0.106	—	0.98	—	—	0	< 0	—
4.0	13	1.33	0.106	0.073	0.87	0.71	—	0	< 0	—
4.0	13	0.67	0.106	—	0.72	—	—	0	< 0	±21
4.0	23	2.00	0.108	—	0.79	—	—	0	< 0	±16
4.0	23	1.33	0.108	0.060	0.69	0.61	—	0	< 0	±12
4.0	23	0.67	0.108	—	0.51	—	—	0	< 0	±10
3.0	0	2.00	0.106	—	0.96	—	—	13	> 0	—
3.0	0	1.33	0.106	0.068	0.91	0.75	0.74	15	> 0	—
3.0	0	0.67	0.106	—	0.81	—	—	20	> 0	—
3.0	13	2.00	0.107	—	0.90	—	—	0	< 0	—
3.0	13	1.33	0.107	0.067	0.84	0.70	0.71	0	< 0	±31
3.0	13	0.67	0.107	—	0.70	—	—	0	< 0	±30
3.0	23	2.00	0.109	—	0.82	—	—	0	< 0	—
3.0	23	1.33	0.109	0.060	0.76	0.66	0.61	0	< 0	±22
3.0	23	0.67	0.109	—	0.59	—	—	0	< 0	±20
2.4	0	2.00	0.108	—	0.91	—	—	23	> 0	—
2.4	0	1.33	0.108	0.058	0.83	0.71	—	23	> 0	—
2.4	0	0.67	0.108	—	0.71	—	—	14	> 0	—
2.4	13	2.00	0.107	—	0.88	—	—	17	> 0	—
2.4	13	1.33	0.107	0.058	0.78	0.68	—	16	> 0	—
2.4	13	0.67	0.107	—	0.63	—	—	20	> 0	—
2.4	23	2.00	0.107	—	0.81	—	—	0	< 0	—
2.4	23	1.33	0.107	0.058	0.74	0.65	—	0	< 0	±27
2.4	23	0.67	0.107	—	0.57	—	—	0	< 0	±25

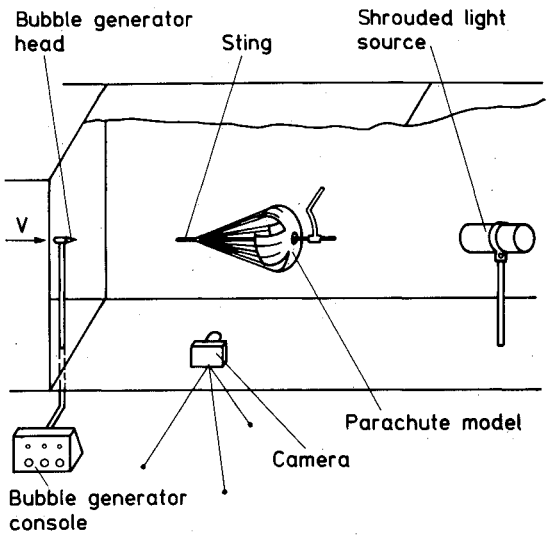

Fig. 5 Experimental arrangement for helium-bubble visualization.

where the bubbles are ejected into the airstream is shown: the quantities of helium, air, and soap solution can be adjusted at the control console. This figure also shows the shrouded light source downstream and the camera, the latter being located outside the working section. Success or failure in obtaining satisfactory photographic records is heavily dependent on the intensity, narrowness of field of view, and duration of the light source selected.

Results Obtained

Values for the tangential force coefficient at zero angle of attack C_{To}, the angle of attack at which the canopy is both in equilibrium and is statically stable α_{eq}, the maximum angle of attack α_{col} at which the canopy is fully inflated and without collapse, together with the sign of the rate of change of the pitching moment coefficient about the suspension line confluence point with the angle of attack, $dC_{Mc}/d\alpha$ at zero angle of attack, are all listed in Table 2. All coefficients are based on the nominal total surface area S_o.

There was a significant blockage constraint for the parachute canopies in the wind tunnel working section, for which the blockage factor based on canopy projected area was between 6% and 8%. As part of an experimental program conducted by Cockrell et al.,[7] steady values for C_{To} were also determined using data obtained from ship tank tests. In these latter tests the model canopies were immersed in water and mounted via a strain-gaged sting to a towing carriage. This carriage traveled with a velocity of some 1.5 m/s down the 61 m (200 ft) length of the 3.66×1.83 m (12×6 ft) tank, in which the model blockage factor was only about 1.0%.

Corrections for blockage constraint can be made to measured values of force and moment coefficients using the methods outlined in Ref. 8. Maskell's[9] drag coefficient correction ΔC_D is expressed there as

$$\frac{\Delta C_D}{C_D} = -2.77 C_D \frac{S}{A} \tag{1}$$

where the blockage ratio S/A is the ratio of body cross-sectional area to that of the test facility in which it is placed. The corresponding across-flow force coefficient blockage correction ΔC_c is

$$\frac{\Delta C_c}{C_c} \sim -0.2 \frac{S}{A} \tag{2}$$

and even when the blockage ratio is as high as 8% this latter blockage correction has a negligible effect on normal force and pitching moment coefficients. Having applied Eq. (1) to the tangential force coefficient values obtained in the wind tunnel, as Table 2 shows, they agreed acceptably well with corresponding measurements made under water in the much larger cross-sectional area ship tank.

Effects of Canopy Arm Ratio and Porosity on the Tangential Force Coefficient C_T

As the canopy arm ratio increases from 2.4 to 4.0, Fig. 6 shows that the tangential force coefficient at zero angle of attack, C_{To}, also increases. Table 2 shows that with the increase in arm ratio there is also an increase in the canopy projected area S_p for a constant nominal surface area S_o: this is the main cause of the drag increase. Clearly, cross-shaped canopies having high arm ratios are effective drag producers, but they do have a disadvantage. They tend to collapse at lower angles of attack than do smaller arm ratio cross canopies. In Fig. 7, the effect on C_T of increasing the canopy fabric porosity is shown. As Figs. 8 and 9 indicate, this reduction is caused by flow changes around the canopy and these are discussed below.

From Fig. 10 it is seen that when cross parachute canopies are caused to rotate by their lack of uniformity at rates up to some three revolutions per second their tangent force coefficients are only marginally higher than when there is no rotation. From flow visualization studies, it is difficult to see any significant change in the flow characteristics which may have been caused by this rotation.

Over the Reynolds number range from 2.0×10^5 to 5.0×10^5 Fig. 11 indicates that the measured tangent force coefficient increases by less than 10%. Ludtke[10] has shown that this increase is even less significant at higher Reynolds numbers. For cross parachutes at Reynolds numbers which are above 10^5 therefore, Reynolds number variation has a negligible

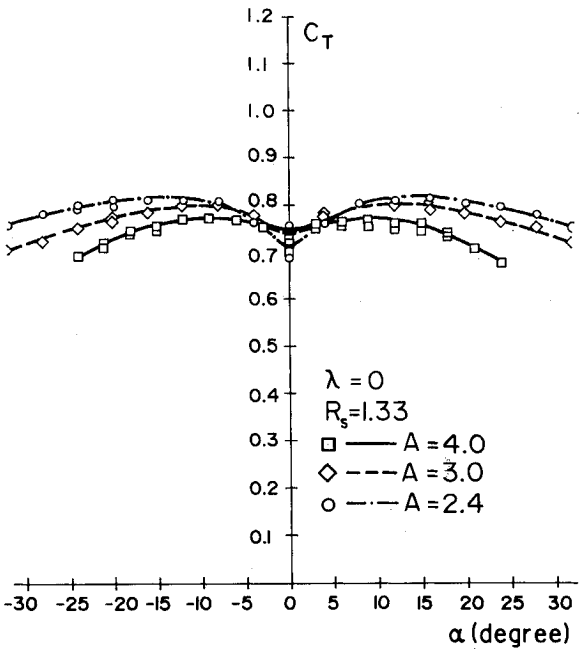

Fig. 6 Variation of tangent coefficient C_T with angle of attack α for various arm ratios A.

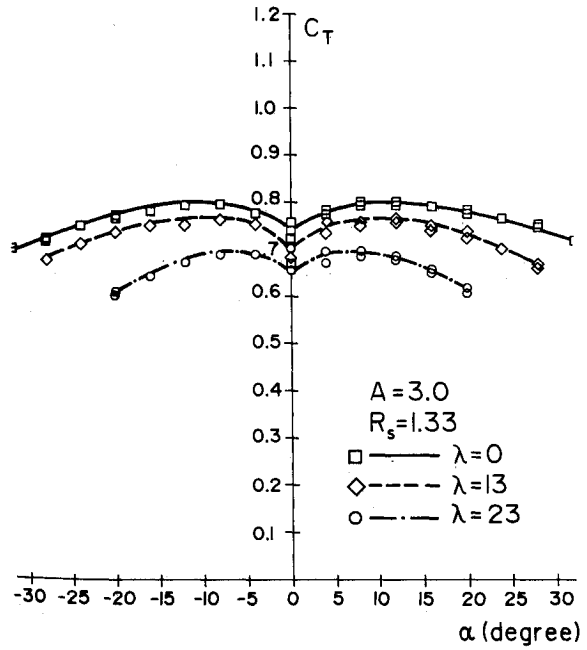

Fig. 7 Variation of tangent coefficient C_T with angle of attack α for various porosities λ.

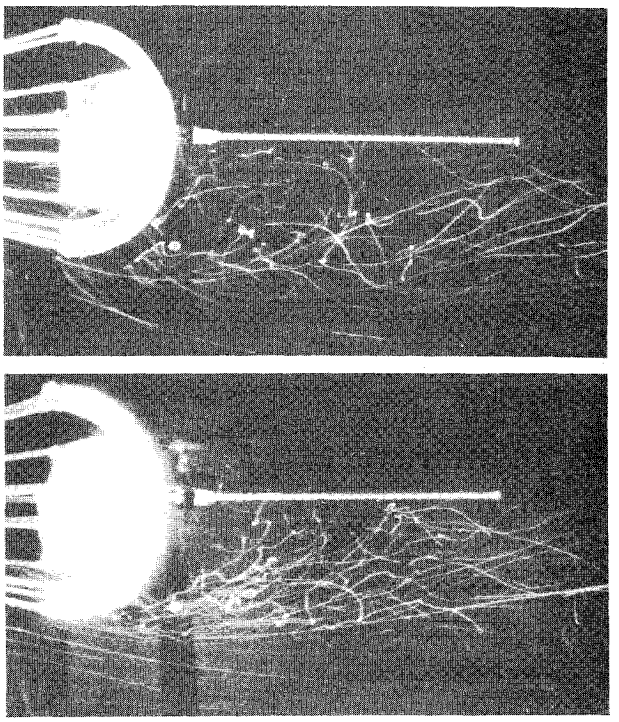

Fig. 8 Flow visualization. 3:1 arm ratio cross canopy: a) imporous canopy, b) highly porous canopy.

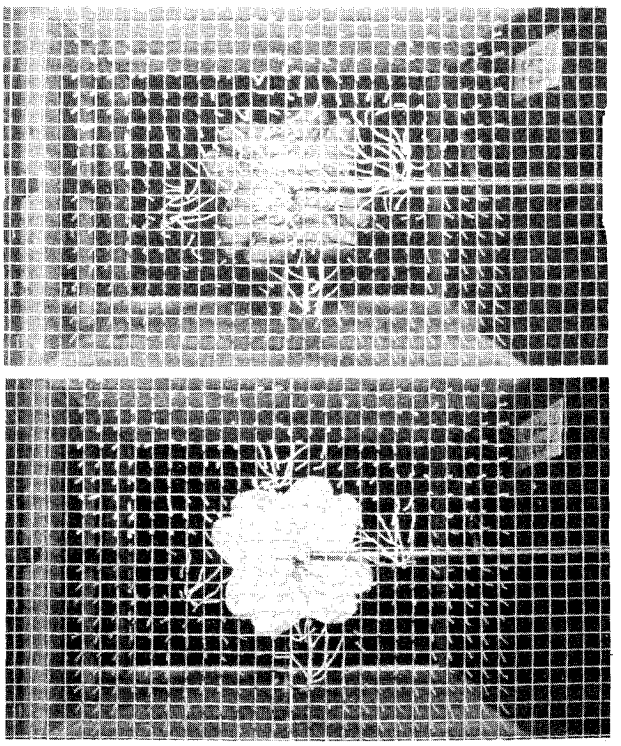

Fig. 9 Wool tufts 150 mm downstream of 3:1 arm ratio cross canopy: a) imporous canopy, b) highly porous canopy.

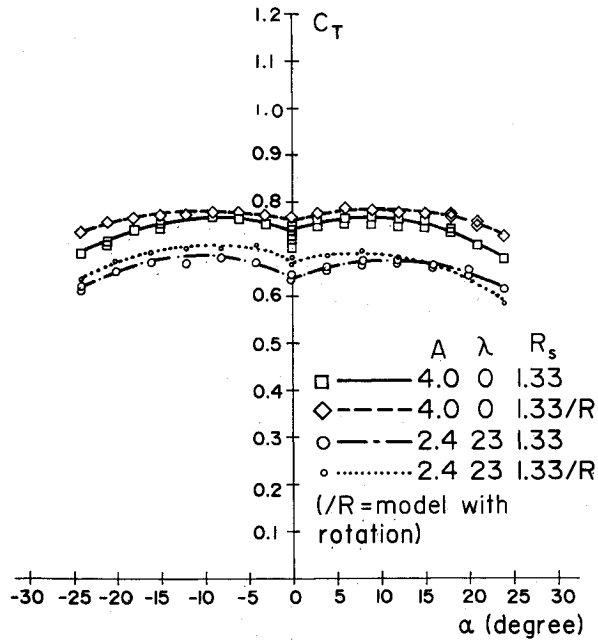

Fig. 10 Effect of canopy rotation on tangent coefficient C_T.

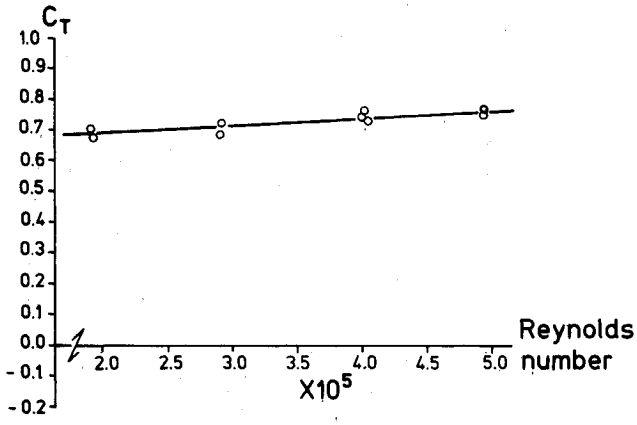

Fig. 11 Variation of tangent coefficient for cross canopies with Reynolds number.

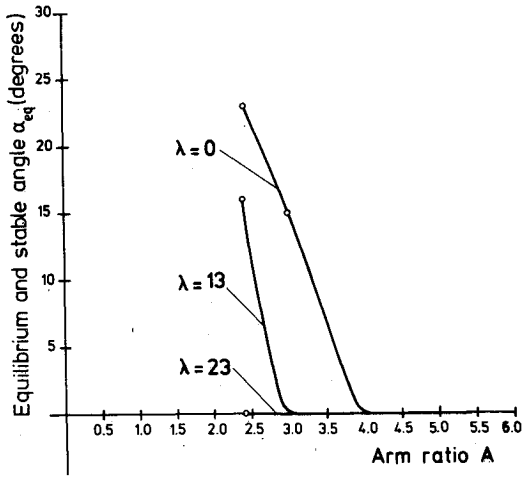

Fig. 12 Variation of equlibrium and stable angle of attack α_{eq} with arm ratio A and porosity λ.

effect on the values of the tangent force coefficient and the drag coefficient.

Effects of Arm Ratio and Canopy Porosity Variation on Cross Canopy Stability Characteristics in Pitch

The criterion for static stability in pitch is that at equilibrium, when $C_N = 0$,

$$\frac{dC_{Mc}}{d\alpha} = -(x_c - x_p)\frac{dC_N}{d\alpha} < 0 \qquad (3)$$

The equilibrium and statically stable angles of attack are shown in Fig. 12 to be functions of both canopy arm ratio A and porosity λ. Since an inspection of Figs. 13 and 14 reveals that $dC_N/d\alpha$ at $\alpha = 0$ deg becomes increasingly positive as the canopy arm ratio or as the porosity of the canopy fabric is made larger, the static stability of cross parachutes is increased as arm ratios and canopy porosities are made greater. Further, since Doherr and Saliaris[11] have shown that the single most important condition for dynamic stability in pitch is that this static stability criterion is strongly established, Figs. 13 and 14 indicate that certain combinations of arm ratio and porosity will ensure dynamically stable pitching motion. It is also possible for canopies with weakly positive values of $dC_{Mc}/d\alpha$ at equilibrium to exhibit dynamic stability in pitch; this point has been further discussed by Cockrell et al.[7]

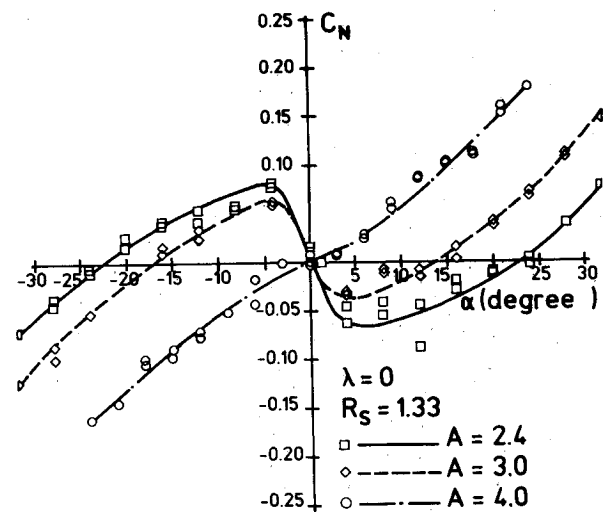

Fig. 13 Variation of normal coefficient C_N with angle of attack α for various arm ratios A.

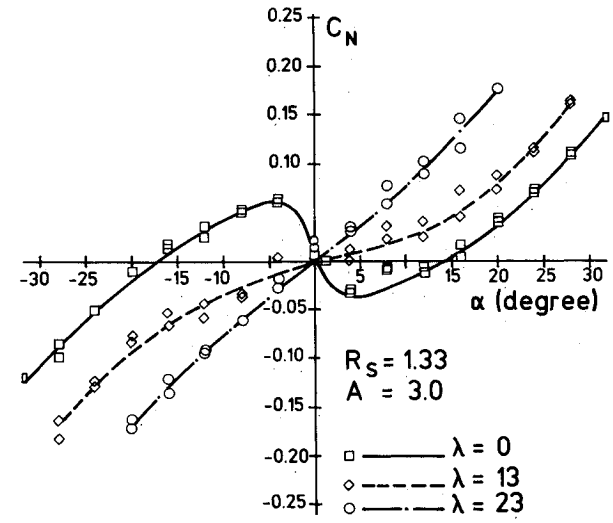

Fig. 14 Variation of normal coefficient C_N with angle of attack α for various porosities λ.

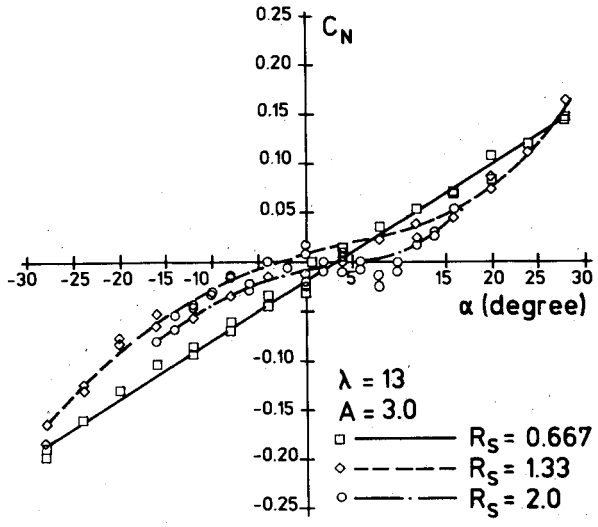

Fig. 15 Effect of suspension line ratio on the static stability criterion.

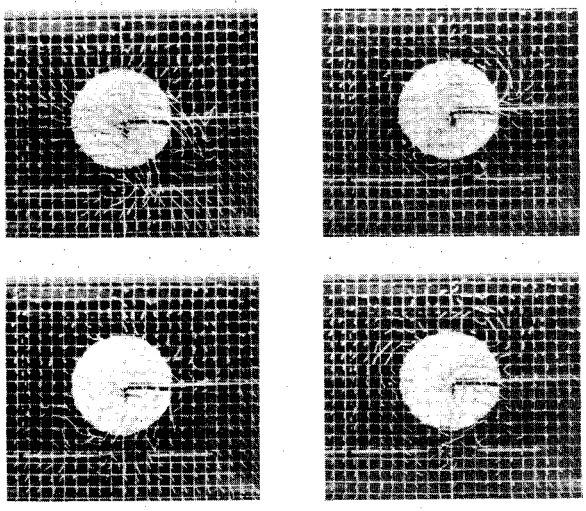

Fig. 16 Wake characteristics shown by wool tufts downstream of a round canopy.

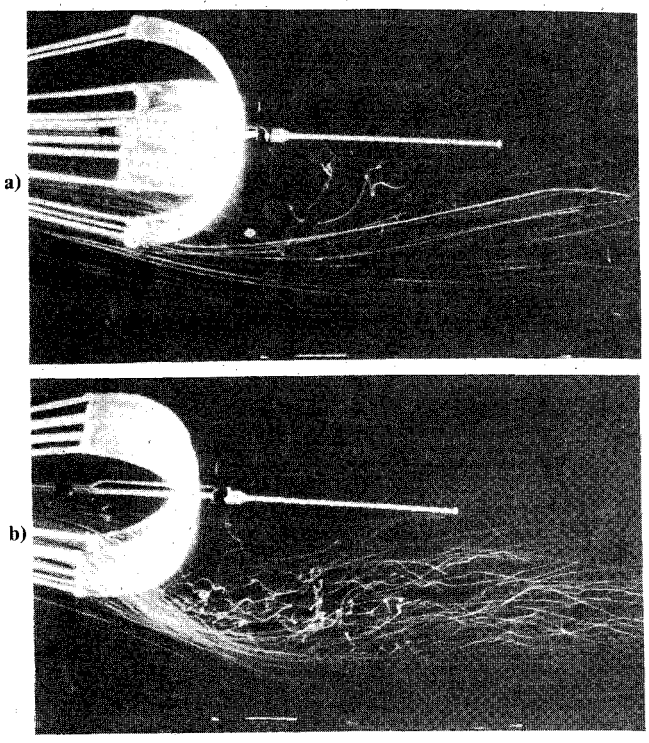

Fig. 17 Flow visualization around a 4:1 arm ratio cross canopy: a) flow over arm, b) flow through gap.

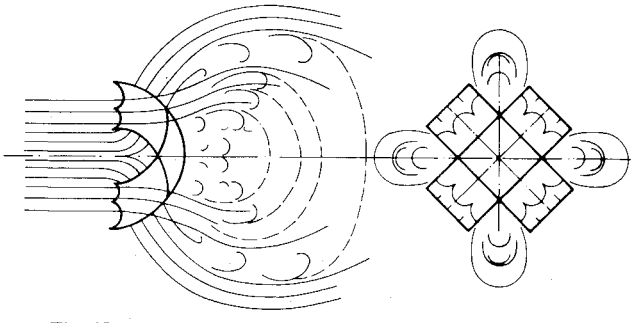

Fig. 18 The flow around and downstream of a cross canopy.

Effects of the Suspension Line Ratio Variation on Aerodynamic Characteristics

An increase in tangential force coefficient is observed when the suspension line ratio is increased, but as Fig. 15 shows, this increase has very little effect on $dC_N/d\alpha$.

Discussion of Flow Characteristics Around Cross-Shaped Canopies

From the studies of the flow around a sphere which Taneda[3] made, it can be seen that the wake rolls up into a pair of randomly orientated vortex rings. The four successive frames of photographs taken with a motor-driven camera and shown in Fig. 16 reveal that in the wake formed behind a round parachute canopy at zero angle of attack there is the same random orientation, resulting in an aerodynamic normal force component which has zero mean value but which fluctuates at the frequency of the wake motion. Although more pronounced with a round canopy than with cross canopies, Shen[12] has observed the same fluctuations in the normal forces developed by cross parachute canopies.

Figure 17 shows that differences occur in the flow through the gaps formed between the cross canopy arms and the flow across these arms.

Flow through the gaps can be seen in Fig. 17b. As this stream flows into the canopy, it decelerates and loses energy by mixing. Then, it accelerates through the gap to the canopy upper surface, going on to join the downstream wake. Since the fluid which it joins has also lost energy by mixing, it does little to raise or lower speeds in the wake, but its main effect, which can be observed from the direction of the free streamline in Fig. 17b, is to widen the wake in the manner shown by the sketch of Fig. 18.

The flow over the arms separates from the canopy long before reaching the apex. The point of separation varies both with the canopy arm ratio and with the porosity of its fabric. With the 4:1 arm ratio imporous canopy shown in Fig. 17a there is some flow attachment near the hem of the canopy skirt. However, flow around the 3:1 arm ratio imporous canopy shown in Fig. 8a does not appear to be attached. In the photographs of 3:1 arm ratio canopies shown in Figs. 8a and 8b the position of flow separation is strongly dependent on the porosity of the canopy. As Fig. 9 shows that the earlier the position of flow separation the wider the wake becomes, the canopy porosity is seen to have a marked effect on the drag characteristics.

The flow visualization photographs shown in Fig. 19 and in Fig. 8 reveal that the stability of cross canopies is dependent on the ability of the air otherwise trapped within the canopy to flow out freely, both through the gaps which are formed between the canopy arms and through the canopy fabric. When all these gaps are small, for example when the arm ratio A equals 2.4 or 3.0, and the fabric is imporous, some of this enclosed air spills out, like tea from a cup, around the hem of

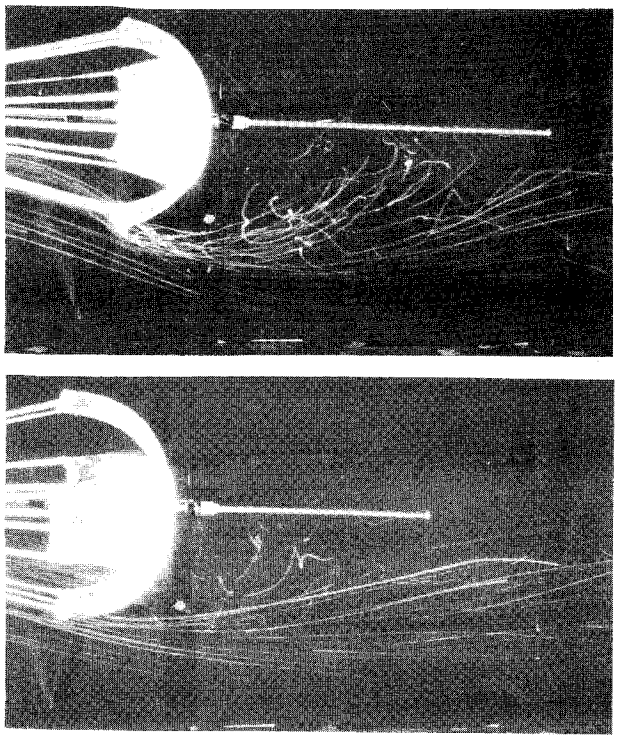

Fig. 19 Flow visualization over the arm of imporous cross canopies $\alpha = 0$ deg: a) arm ratio 2.4:1, b) arm ratio 4.0:1.

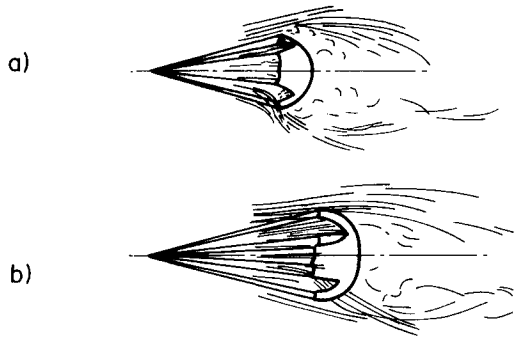

Fig. 20 Flow visualization over the arm of imporous cross canopies $\alpha = 5$ deg: a) arm ratio 2.4:1, b) arm ratio 4.0:1.

the canopy skirt and produces a destabilizing moment. Increasing the arm ratio or the porosity of the canopy will reduce this destabilizing tendency.

When disturbed from equilibrium at zero angle of attack the characteristics of the flows around canopies having arm ratios of 2.4:1 and 4.0:1 are shown in Fig. 20. In Fig. 20a the direction in which the entrapped air spills out of the inside of the 2.4:1 arm ratio canopy results in a destabilizing aerodynamic moment, whereas in Fig. 20b the flow pattern from the 4.0:1 arm ratio canopy gives an aerodynamic moment which is in a stabilizing direction.

Conclusions

1) Cross parachute canopies having arm ratios $A = L/W$ of 4:1 possess excellent static and dynamic stability characteristics in pitch. They also possess high drag characteristics (C_{To}).

2) Cross parachute canopies having arm ratios of 3:1 possess good stability and drag characteristics, provided that they are not manufactured from an imporous fabric.

3) Cross parachute canopies having an arm ratio of 2.4:1 do not possess good stability characteristics at zero angle of attack.

4) Although the aerodynamic characteristics of cross parachute canopies are mainly dependent on arm ratio, fabric porosity does play a significant role. An increase in canopy porosity will result in a decrease in drag and an increase in stability and pitch; an increase in arm ratio results in an increase in both drag and stability.

5) Over a Reynolds number range from 2.0×10^5 to 5.0×10^5 the observed variation in C_{To} was less than 10%.

6) Values of drag obtained with a substantial wind tunnel blockage factor, based on canopy projected area, of about 7.5% can be satisfactorily compensated for by application of Maskell's bluff body correction factor, but blockage factors much greater than 5% are not to be recommended.

7) The flow in the wake behind cross-shaped canopies is complex. Although mean flows are steady, the random fluctuations caused by vortex rings present in the wake casue randomly fluctuating instantaneous aerodynamic forces to be developed on the canopy.

8) The suspension line ratios $R_s = \ell_s/L$ giving the most satisfactory aerodynamic and stability characteristics lie between 1.0 and 1.5.

Acknowledgments

The experimental work on which this paper is based was supported by Irvin Great Britain Ltd. The authors express their thanks to the company and to Mr. M. Harper-Bourne, the chief designer, for all his encouragement and help. The views expressed are the authors' own.

References

[1]Jorgensen, D.S., D.S., "Cruciform Parachute Aerodynamics," Ph.D. Thesis, Univ. of Leicester, Leicester, U.K., 1982.

[2]Ludtke, W.P., "Effects of Canopy Geometry on the Spinning Characteristics of a Cross Parachute with a W.L. Ratio of 0.264," U.S. Naval Ordnance Laboratory, NOLTR 72-145, June 1972.

[3]Taneda, S., "Visual Observations of the Flow Past a Sphere at Reynolds Numbers Between 10^4 and 10^6," *Journal of Fluid Mechanics*, Vol. 85, 1978, pp. 187–192.

[4]Bearman, P.W. and Trueman, D.M., "An Investigation of the Flow Around Rectangular Cylinders," *Aeronautical Quarterly*, Vol. 23, Aug. 1972, pp. 229–237.

[5]Nakamura, Y. and Ohya, Y., "Vortex Shedding From Square Prisms in Smooth and Turbulent Flows," *Journal of Fluid Mechanics*, Vol. 164, 1986, pp. 77–89.

[6]Knacke, T.W., "Decelerator Systems Engineering," Proceedings, Univ. of Minnesota Decelerator Systems Engineering Short Course, Albuquerque, NM, July 1985.

[7]Cockrell, D.J., Shen, C.Q., Harwood, R.J., and Baxter, A.C., "Aerodynamic Forces Acting on Parachutes in Unsteady Motion and the Consequential Dynamic Stability Characteristics," AIAA Paper 86-2470-CP, Oct. 1986.

[8]"Blockage Corrections for Bluff Bodies in Confined Flows," Item No. 80024, Engineering Sciences Data Unit, London, U.K. 1976.

[9]Maskell, E.C., "A Theory of the Blockage Effects on Bluff Bodies and Stalled Wings in a Closed Wind Tunnel," ARC R&M 3120, U.K. Aeronautical Research Council, Nov. 1965.

[10]Ludtke, W.P., "Effects of Canopy Geometry on a Cross Parachute, in the Fully Open and Reefed Conditions, for a W:L Ratio of 0.264," U.S. Naval Ordnance Laboratory, NOLTR 71–111, Aug. 1971.

[11]Doherr, K.-F. and Saliaris, C., "On the Influence of Stochastic and Acceleration Dependent Aerodynamic Forces on the Dynamic Stability of Parachutes," AIAA Paper 81-1941. Oct. 1981.

[12]Shen, C.Q., "Flow Field Characteristics Around Bluff Parachute Canopies," Ph.D. Thesis, Leicester Univ., Leicester, U.K., June 1987.